

Article

Integrated Electro-Ozonation and Fixed-Bed Column for the Simultaneous Removal of Emerging Contaminants and Heavy Metals from Aqueous Solutions

Amin Mojiri ^{1,*}, Noriatsu Ozaki ^{1,*}, John L. Zhou ², Reza Andasht Kazeroon ³, Mohammad Ali Zahed ⁴, Shahabaldin Rezania ⁵, Mohammadtaghi Vakili ⁶, Shahin Gavanji ⁷ and Hossein Farraji ⁸

¹ Department of Civil and Environmental Engineering, Graduate School of Advanced Science and Technology, Higashihiroshima 739-8725, Japan

² School of Civil and Environmental Engineering, University of Technology Sydney, Sydney, NSW 2007, Australia

³ Faculty of Civil Engineering, Xi'an University of Architecture and Technology, Xi'an 710055, China

⁴ Faculty of Biological Sciences, Kharazmi University, Tehran 15719-14911, Iran

⁵ Department of Environment and Energy, Sejong University, Seoul 05006, Korea

⁶ Green Intelligence Environmental School, Yangtze Normal University, Chongqing 408100, China

⁷ Department of Biotechnology, Faculty of Advanced Sciences and Technology, University of Isfahan, Isfahan 81746-73441, Iran

⁸ School of Physical and Chemical Sciences, University of Canterbury, Christchurch 8140, New Zealand

* Correspondence: amin.mojiri@gmail.com (A.M.); ojaki@hiroshima-u.ac.jp (N.O.)



Citation: Mojiri, A.; Ozaki, N.; Zhou, J.L.; Kazeroon, R.A.; Zahed, M.A.; Rezania, S.; Vakili, M.; Gavanji, S.; Farraji, H. Integrated Electro-Ozonation and Fixed-Bed Column for the Simultaneous Removal of Emerging Contaminants and Heavy Metals from Aqueous Solutions. *Separations* **2022**, *9*, 276. <https://doi.org/10.3390/separations9100276>

Academic Editor: Qicheng Feng

Received: 30 August 2022

Accepted: 29 September 2022

Published: 1 October 2022

Publisher's Note: MDPI stays neutral with regard to jurisdictional claims in published maps and institutional affiliations.



Copyright: © 2022 by the authors. Licensee MDPI, Basel, Switzerland. This article is an open access article distributed under the terms and conditions of the Creative Commons Attribution (CC BY) license (<https://creativecommons.org/licenses/by/4.0/>).

Abstract: In the current study, an integrated physiochemical method was utilized to remove tonalide (TND) and dimethyl phthalate (DMP) (as emerging contaminants, ECs), and nickel (Ni) and lead (Pb) (as heavy metals), from synthetic wastewater. In the first step of the study, pH, current (mA/cm²), and voltage (V) were set to 7.0, 30, and 9, respectively; then the removal of TND, DMP, Ni, and Pb with an electro-ozonation reactor was optimized using response surface methodology (RSM). At the optimum reaction time (58.1 min), ozone dosage (9.4 mg L⁻¹), initial concentration of ECs (0.98 mg L⁻¹), and initial concentration of heavy metals (28.9 mg L⁻¹), the percentages of TND, DMP, Ni, and Pb removal were 77.0%, 84.5%, 59.2%, and 58.2%, respectively. For the electro-ozonation reactor, the ozone consumption (OC) ranged from 1.1 kg to 3.9 kg (kg O₃/kg Ecs), and the specific energy consumption (SEC) was 6.95 (kWh kg⁻¹). After treatment with the optimum electro-ozonation parameters, the synthetic wastewater was transferred to a fixed-bed column, which was filled with a new composite adsorbent (named BBCEC), as the second step of the study. BBCEC improved the efficacy of the removal of TND, DMP, Ni, and Pb to more than 92%.

Keywords: dimethyl phthalate; electrochemical oxidation; ozone; nickel; tonalide

1. Introduction

Efforts to maintain the quality of water are facing severe challenges due to increasing water consumption and usage worldwide [1]. Industrialization, urbanization, and a growing population have led to a decline in the quantity and quality of water bodies [2]. The main sources of water contamination are industrial and agricultural wastes, which contain various toxics, including heavy metals and organic pollutants (such as emerging contaminants), and have been released into water bodies [1].

The global output of emerging contaminants (ECs) has been predicted to increase from 1 million to 500 million tons each year. ECs endanger human health and the environment [3]. Tonalide (TND), 6-acetyl-1,1,2,4,4,7-hexamethyltetraline (AHTN), is one of the largest polycyclic musk products, representing approximately 95% of the EU market and 90% of the US market [4]. In one study, up to 1.9 mg L⁻¹ of TND was reported in a wastewater treatment plant (WWTP) [5]. TNDs are highly persistent compounds that can accumulate in the environment and the food chain, thereby posing a risk to human

health [6]. Dimethyl phthalate (DMP) has been significantly employed as a plasticizer in the industrial process, and is widely reported to be in various aquatic environments (such as drinking water) [7]. In European countries, the concentration of DMP in landfill leachate has reached 300 mg L^{-1} [8].

Heavy metals are another type of contaminant that have been released into water bodies due to industrial and agricultural activities. Heavy metals are posing a risk to human health and the environment due to bioaccumulation, persistence, and environmental toxicity [9]. Nickel (Ni^{2+}) is regularly used in numerous industrial activities (such as electroplating, ceramic coloring, forging, mineral processing, steam-electric power generation, and production of metallic alloys) due to its high-temperature stability, toughness, ductility, strength, and corrosion resistance [10]. Lead (Pb^{+2}) ions are among the most harmful heavy metal ions reported in water bodies, having carcinogenic and various other antagonistic impacts on tissues and living organisms [11]. The concentrations of Pb and Ni in water bodies could reach hundreds of mg L^{-1} [12].

Several studies have stated that wastewater treatment plants (WWTPs) cannot remove ECs and heavy metals efficiently [12,13]; thus, researchers have tried to introduce new treatment methods. Adsorption and advanced oxidation processes (AOPs) are considered efficient ways to deal with refractory organic contaminants and heavy metals [2,13,14]. AOPs generate highly reactive radical oxidative species (ROS), such as hydroxyl radicals ($\bullet\text{OH}$), ozone (O_3), and hydrogen radicals ($\bullet\text{H}$), which can be highly efficient in the elimination of recalcitrant contaminants [15]. Among the AOP methods, electrochemical oxidation and ozonation have attracted the attention of researchers. During the treatment of organic pollutants by ozonation, the oxidation and breaking down of pollutants occur either by ozone (O_3) molecules directly and/or by indirect degradation via hydroxyl radical activity. However, several studies [16] have stated that the emerging contaminants can be only removed partially by ozonation. The main drawback of ozonation is associated with low mineralization, which may lead to the production of intermediates with toxic features [17]. Therefore, several researchers [18,19] have tried to integrate the ozone reactor with other methods. One of the methods that is combined with ozonation is electrochemical oxidation; however, the integration of electrochemical oxidation and ozonation is mostly accomplished in sequencing reactors [20,21]. In the current study, electrochemical oxidation (EO) and ozonation were run in a single reactor simultaneously to enhance the mineralization of organic contaminants, improve the effects of ozonation and electrochemical oxidation, and reduce the production of intermediates compounds. Alfonso-Muniozguren et al. [20] stated that EO with non-active electrodes (such as boron-doped diamond, BDD) enhances the production of free hydroxyl radicals ($\bullet\text{OH}$), which are helpful in breaking down the high-molecular-weight, persistent organic contaminants. A promising method that combines with AOPs and removes emerging contaminants is the adsorption technique. Several efficient adsorbents (such as clay, activated carbon, biochar, and lime) have been reported to be effective in eliminating emerging contaminants and heavy metals [22]. For the removal of contaminants from water bodies, biochar-based adsorbent has attracted attention because of its properties, including a porous structure, a large specific surface area, and enriched surface functional groups [23,24]. Apart from that, cockleshell, eggshell, and bentonite can be effective in the ion exchange during the removal of contaminants. A composite adsorbent can retain the properties and advantages of its components, which means it would be of more use than its parts in the removal of contaminants [25]. Therefore, a novel composite adsorbent has been produced and used in this study.

As a summary, the study was aimed at: (1) removing emerging contaminants and heavy metals using a hybrid method (including electrochemical oxidation, ozonation, and fixed-bed column); and (2) introducing a new composite adsorbent.

2. Materials and Methods

TND ($\text{C}_{18}\text{H}_{26}\text{O}$, CAS: 21145-77-7, molecular weight 258.4 g/mol), DMP ($\text{C}_6\text{H}_4(\text{COOCH}_3)_2$, CAS: 131-11-3, molecular weight 194.1 g/mol), nickel (II) sulfate hexahydrate ($\text{NiSO}_4 \cdot 6\text{H}_2\text{O}$,

CAS: 10101-97-0) [26], and lead (II) nitrate ($\text{Pb}(\text{NO}_3)_2$, CAS: 10099-74-8) [27] were purchased from Sigma-Aldrich. Biochar (derived from wheat straw with pyrolysis at $550\text{ }^\circ\text{C}$), bentonite, cockleshells, Portland cement, and eggshells were collected from local shops.

In this study, two reactors were employed based on the diagram in Figure 1. In the first step, synthetic wastewater was treated using an electro-ozonation reactor. The wastewater was then moved through a fixed-bed column (with flow rate of 1 mL min^{-1} [28]) for further treatment with a composite adsorbent.

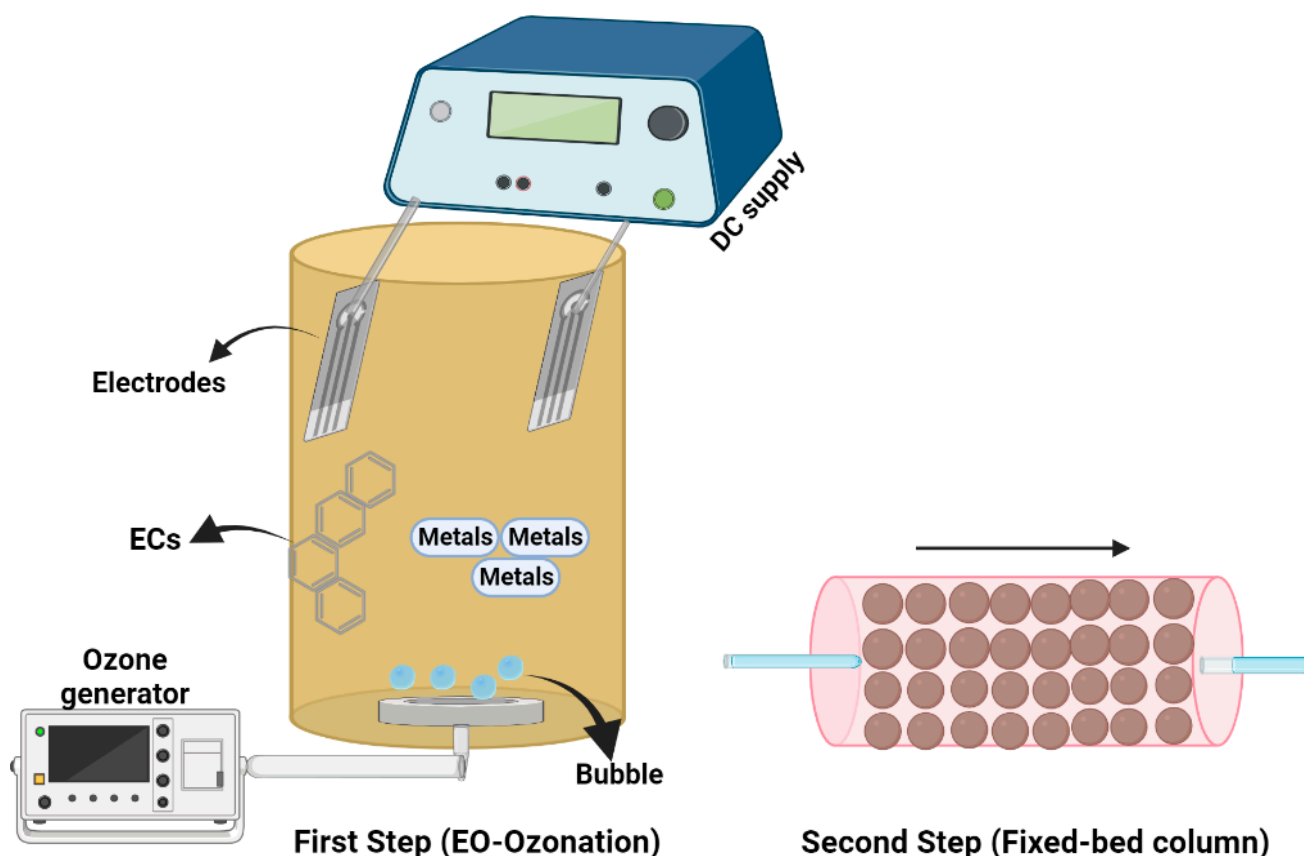


Figure 1. Schematic of the reactors.

2.1. Synthetic Wastewater

A stock standard solution of TND and DMP was obtained by dissolving them in methanol and keeping the resulting solution at $4\text{ }^\circ\text{C}$. Different concentrations of TND and DMP were produced before the experiments through dilution of stock standard solutions with a mixture of methanol:water (50:50, *v/v*) [13]. The EC concentrations varied from 0.2 to 1.2 mg L^{-1} . In addition, to reach the concentrations of Ni (II) and Pb (II) in wastewater, the stock solution of Ni (II) and Pb (II) was diluted to reach the concentration (10 to 60 mg L^{-1}). The pH of synthetic wastewater was adjusted to neutral with HCl and NaOH [29].

2.2. Electro-Ozonation Reactor

A cylinder with a diameter of 11 cm and a height of 50 cm (a volume of 4.7 L) was applied as the ozone reactor. To improve the ozone gas diffusion, a cross-column ozone chamber was employed at the bottom of the reactor. To produce ozone, an ozone generator (BMT Messtechnik, Germany) fed with dry oxygen was employed. In addition, an ultraviolet gas ozone detector (Lontec, Qingdao) was applied to measure the ozone dosage. To keep the reflex temperature at $<15\text{ }^\circ\text{C}$ and to reach the optimum half-life of the dissolved ozone in water, a water bath and a cooling system were used. The ozone

doses and ozonation times (reaction time, min) were 5 to 30 mg L⁻¹, and 10 to 60 min, respectively, which are in line with findings of [29,30].

At the top of the ozone reactor, boron-doped diamond (BDD, 18 cm × 8 cm) and Ti/RuO₂ (18 cm × 8 cm) as the anode and cathode, respectively, were placed parallel at a distance of 3 cm [30]. Electronic power (Digital CC&CV DC Power Supply, Everfine, Hangzhou, China) was applied to reach the current (30 mA/cm²) and voltage (9 V) achieved in the preliminary experiments, which are in line with findings of [30–32]. NaCl (50 mM) was added to the synthetic wastewater as the electrolyte [33].

2.3. Composite Adsorbent

The fixed-bed column was filled with a novel powdered composite adsorbent (BBCEC, which included biochar, bentonite, cockleshell, eggshell, and cement). The biochar, cockleshell, and eggshell were ball-milled, and then passed through a sieve (300 μm mesh). These powdered materials were then mixed with bentonite powder and Portland cement after adding sufficient tap water. Subsequently, a mold was filled with the mixture. After 48 h, the adsorbent (BBCEC) was removed from the mold and soaked in a water pond for 24–48 h. Next, the BBCEC was air-dried and crushed into powder. The results of the XRF (X-ray fluorescence) analysis of BBCEC are displayed in Table 1. Based on autosorb (Quantachrome IQ, Germany) analysis, the BET surface (m²/g), micropore volume (cc/g), micropore area (m²/g), and Langmuir surface area (m²/g) were 256, 30.2, 129, and 521, respectively.

Table 1. XRF analysis of BBCEC.

Compounds/Elements	Composition (%)	Compounds/Elements	Composition (%)
C	15.6	K ₂ O	1.2
CaO	38.9	MgO	1.0
SiO ₂	34.7	Na ₂ O	1.0
Al ₂ O ₃	5.1	SO ₃	0.5
Fe ₂ O ₃	1.6	Others	0.4

2.4. Optimization Process and Statistical Analysis

The effectiveness of the removal of heavy metals and emerging contaminants was evaluated based on Equation (1). The optimization process was carried out using response surface methodology (RSM) and central composite design (CCD) through DOE 10.0.7 software with four independent factors: ozonation time (reaction time, min), ozone dosage (mg L⁻¹), initial concentration of ECs (mg L⁻¹), and initial concentration of heavy metals (mg L⁻¹). As there were three levels for each factor, the suitable model was the quadratic (Equation (2)). Each experiment was carried out with three replications. The model terms were assessed using P-value (probability) with a 95% confidence level [34].

$$\text{Removal (\%)} = \frac{\text{Initial concentration } \left(\frac{\text{mg}}{\text{L}}\right) - \text{final concentration } \left(\frac{\text{mg}}{\text{L}}\right)}{\text{Initial concentration } \left(\frac{\text{mg}}{\text{L}}\right)} \times 100 \quad (1)$$

$$Y = \beta_0 + \sum_{j=1}^k \beta_j X_j + \sum_{j=1}^k \beta_{jj} X_j^2 + \sum_i \sum_{<j=2}^k \beta_{ij} X_i X_j + e_i \quad (2)$$

Here, the response is shown by Y; the variables are represented by X_i and X_j; the interaction coefficients of the linear, quadratic, and second-order terms are denoted by β_j, β_{jj}, and β_{ij}, respectively; and e denotes error.

2.5. Analysis of Ozone Consumption (OC) and Specific Energy Consumption (SEC)

Equation (3) (modified from [30]) was used to calculate ozone consumption through the removal of certain amounts of ECs by ozonation:

$$OC = \frac{Q_G}{V} \times \frac{\int_0^t \left(1 - \frac{C_{AG}}{C_{AG0}}\right) dt}{EC_0 - EC} \tag{3}$$

where the gas flow rate (mL/min) and volume (mL) are denoted by Q_G and V , the input ozone concentration (g m^{-3}) and the off-gas ozone concentration (g m^{-3}) are represented by C_{AG} and C_{AG0} , and the initial and final concentrations of ECs are shown by EC_0 and EC .

The SEC during the removal of ECs via electrochemical oxidation, in batch experiments, was calculated using Equation (4) (modified from [35]):

$$SEC = \frac{E I t}{V (E_0 - E_t)} \tag{4}$$

where the current (A) is denoted by I , volume (L) is demonstrated by V , average of voltage (V) is represented by E , time (h) is presented as t , and EC_0 and EC_t (mg L^{-1}) are the initial concentrations of ECs and the concentrations of ECs in time (t), respectively.

2.6. Study of the Adsorption Isotherm

The adsorption isotherm experiments, with the initial concentrations of TND and DMP (0.2 to 1 mg L^{-1}), and Ni and Pb (10 to 50 mg L^{-1}), at neutral pH, were conducted using Langmuir (Equation (5)) and Freundlich (Equation (6)) isotherm models [36]. For monitoring the isotherm studies, the batch experiments were conducted under different BBCEC dosages (up to 12 g/L) in beakers (with working value of 250 mL). The 1 M HCl or 1 M NaOH solution was applied to adjust the pH. Beakers were shaken at 200 rpm for 24 h .

$$q_e = \frac{q_m K_L C_e}{1 + K_L C_e} \tag{5}$$

$$q_e = K_F C_e^{\frac{1}{n}} \tag{6}$$

where the maximum adsorption capacity is represented by q_m (mg g^{-1}), the equilibrium concentration is demonstrated by q_e (mg g^{-1}), K_L denotes the Langmuir isotherm constant, K_F is the Freundlich constant, predicting the quantity of the adsorbates per gram of adsorbents at the equilibrium concentration, and n refers to a fixed variable signifying the intensity of adsorption.

2.7. Analytical Methods and Experimental Processes

High-performance liquid chromatography (Agilent, Germany, HPLC) with a UV detector and a C18 column was employed to analyze the TND and DMP. The mobile phase included deionized water and methanol (volumetric ratio 30/70). The limit of detection (LOD) was calculated on the basis of $3\sigma/s$ (" σ " is the standard deviation of the peak and " s " is calibration curve) [37]. Ni and Pb were measured using a Hach DR2800 spectrophotometer (Hach Co. Ltd., Loveland, CO, USA).

3. Results and Discussion

In this study, DMP and TND (as the emerging contaminants), and Ni and Pb (as the heavy metals), were removed with electro-ozonation (step 1) and a fixed-bed column (step 2). The removal efficiencies of the electro-ozonation reactor are shown in Table 2. After the treatment of synthetic wastewater with electro-ozonation, the water moved through a fixed-bed column (which was filled with powdered BBCEC).

Table 2. Removal values for different independent factors.

Run	A * (min)	B (mg L ⁻¹)	C (mg L ⁻¹)	D (mg L ⁻¹)	TND Removal (%)	TND Removed (mg L ⁻¹)	DMP Removal (%)	DMP Removed (mg L ⁻¹)	Ni Re- moval (%)	Ni Removed (mg L ⁻¹)	Pb Re- moval (%)	Pb Removed (mg L ⁻¹)
1	10	5	0.2	10	46.7	0.10	53.1	0.106	32.3	3.2	30.4	3.0
2	20	10	0.2	10	49.2	0.10	57.9	0.116	33.8	3.4	31.5	3.2
3	30	15	0.2	10	54.3	0.11	61.7	0.123	35.1	3.5	34.6	3.5
4	40	20	0.2	10	58.8	0.12	66.5	0.133	41.5	4.2	40.2	4.0
5	50	25	0.2	10	65.3	0.13	73.8	0.148	50.3	5.0	49.1	4.9
6	60	30	0.2	10	64.5	0.13	73.3	0.147	51.4	5.1	51.0	5.1
7	10	5	0.4	20	43.6	0.17	52.1	0.208	31.3	6.3	29.8	6.0
8	20	10	0.4	20	51.7	0.21	56.4	0.226	34.5	6.9	32.5	6.5
9	30	15	0.4	20	54.1	0.22	61.1	0.244	39.7	7.9	35.6	7.1
10	40	20	0.4	20	56.4	0.23	64.7	0.259	41.1	8.2	40.8	8.2
11	50	25	0.4	20	57.3	0.23	70.6	0.282	52.9	10.6	51.8	10.4
12	60	30	0.4	20	60.3	0.24	68.2	0.273	53.5	10.7	52.1	10.4
13	10	5	0.6	30	38.4	0.23	46.0	0.276	29.1	8.7	29.4	8.8
14	20	10	0.6	30	42.5	0.26	50.1	0.301	31.8	9.5	30.6	9.2
15	30	15	0.6	30	52.9	0.32	59.8	0.359	34.7	10.4	33.2	10.0
16	40	20	0.6	30	60.4	0.36	66.9	0.401	40.6	12.2	40.3	12.1
17	50	25	0.6	30	63.6	0.38	73.2	0.439	54.3	16.3	53.9	16.2
18	60	30	0.6	30	61.5	0.37	68.6	0.412	56.2	16.9	56.6	17.0
19	10	5	0.8	40	33.3	0.27	41.4	0.331	28.9	11.6	27.6	11.0
20	20	10	0.8	40	42.1	0.34	48.4	0.387	33.9	13.6	31.4	12.6
21	30	15	0.8	40	48.8	0.39	57.8	0.462	47.2	18.9	45.7	18.3
22	40	20	0.8	40	61.4	0.49	66.0	0.528	50.6	20.2	50.6	20.2
23	50	25	0.8	40	66.2	0.53	74.6	0.597	56.3	22.5	55.0	22.0
24	60	30	0.8	40	63.5	0.51	73.4	0.587	58.2	23.3	56.4	22.6
25	10	5	1.0	50	29.4	0.29	40.8	0.408	27.3	13.7	26.8	13.4
26	20	10	1.0	50	39.6	0.40	47.6	0.476	30.4	15.2	29.5	14.8
27	30	15	1.0	50	53.1	0.53	61.7	0.617	40.1	20.1	40.6	20.3
28	40	20	1.0	50	65.3	0.65	74.9	0.749	45.2	22.6	46.8	23.4
29	50	25	1.0	50	71.3	0.71	80.1	0.801	51.7	25.9	49.3	24.7
30	60	30	1.0	50	68.9	0.69	77.6	0.776	56.1	28.1	56.0	28.0
31	10	5	1.2	60	25.7	0.31	35.6	0.427	25.9	15.5	25.4	15.2
32	20	10	1.2	60	40.5	0.49	50.2	0.602	28.6	17.2	27.1	16.3
33	30	15	1.2	60	50.3	0.60	61.1	0.733	45.8	27.5	43.1	25.9
34	40	20	1.2	60	61.1	0.73	72.4	0.869	50.3	30.2	48.6	29.2
35	50	25	1.2	60	67.4	0.81	75.4	0.905	55.3	33.2	54.0	32.4
36	60	30	1.2	60	67.1	0.81	74.8	0.898	56.4	33.8	55.2	33.1

* A = ozonation time (or reaction time, min); B = ozone dosage (mg L⁻¹); C = initial concentration of ECs (TND and DMP each, mg L⁻¹); D = initial concentration of a heavy metal (Ni and Pb separately, mg L⁻¹).

3.1. Removal of ECs and Heavy Metals with the Electro-Ozonation

During the first step (removal of contaminants with electro-ozonation), the maximum elimination of TND, 71.3% (0.71 mg L⁻¹), and DMP, 80.1% (0.801 mg L⁻¹), was reached at the ozonation time of 50 min, the ozone dosage of 25 mg L⁻¹, the initial concentration of ECs of 1.0 mg L⁻¹, and the initial concentration of heavy metals of 50 mg L⁻¹. Furthermore, the minimum abatement of TND, 25.7% (0.31 mg L⁻¹), and DMP, 35.6% (0.427 mg L⁻¹), was reached at the ozonation time of 10 min, the ozone dosage of 5 mg L⁻¹, the initial concentration of ECs of 1.2 mg L⁻¹, and the initial concentration of heavy metals of 60 mg L⁻¹.

Rosal et al. [5] removed 38–20% of musk ketone and the UV filters with ozonation, which is significantly less than in the current study. Amounts of 27.8% of iopromide and 39.5% of 17-alpha-ethinylestradiol were removed via electrochemical oxidation (boron-doped diamond electrode) after 180 min of contact time, which is significantly less than in the current study, due to the combination with electrochemical oxidation in the current study. A total of 79% of TND was removed with a hybrid reactor (including ozonation), which is in line with findings of the current study [38]. Up to 60% of an EC (carbamazepine) was removed with a hybrid reactor (including ozonation) at an ozone concentration of 20 mg L⁻¹ for approximately 2 h [39]. The integration of O₃/UV (O₃ dosage of 15 mg L⁻¹) removed 14–36% of diatrizoate [40], which is considerably less than in the current study (integration of O₃/electrochemical oxidation). In addition, 22% removal was reached in a study about the removal of DMP with ozonation alone [41].

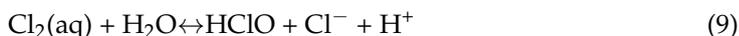
During the first step (contaminant removal with electro-ozonation), the maximum elimination of Ni, 58.2% (23.3 mg L⁻¹), and Pb, 56.4% (22.6 mg L⁻¹), was reached at 60 min of ozonation time, the ozone dosage of 30 mg L⁻¹, the initial concentration of ECs of

0.8 mg L⁻¹, and the initial concentration of heavy metals of 40 mg L⁻¹. Furthermore, the minimum abatement of Ni, 25.9% (15.5 mg L⁻¹), and Pb, 25.4% (15.2 mg L⁻¹), was reached at 10 min of ozonation time, an ozone dosage 5 mg L⁻¹, initial concentration of ECs of 1.2 mg L⁻¹, and the initial concentration of heavy metals of 60 mg L⁻¹. During the Ru/AC catalyzed ozonation of DMP, the maximum removal rate (75%) was reached [42], which is in line with the current study. Mojiri et al. [30] removed 52% of Ni with an integrated method (including electro-ozonation), which is in agreement with the current study.

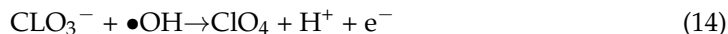
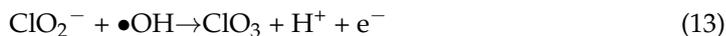
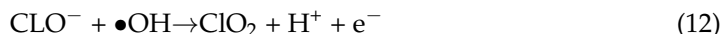
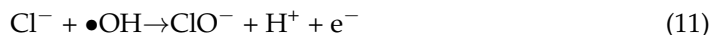
Kanakaraju et al. [43] stated that the BDD electrode is more effective in the removal of ECs due to its high oxygen overpotential (to produce more ^{*}OH radicals), its stability against corrosion, and its inert surface. The high performance of BDD anodes in oxidizing organic substances is attributed to the hydroxyl radicals (^{*}OH radicals) electrogenerated from the water discharge (Equation (7)) [44]:



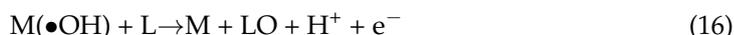
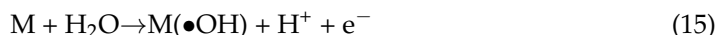
As described by [33], on BDD electrodes, the degradation of organic contaminants can be conducted with two oxidation mechanisms (direct and indirect). Direct oxidation is achieved when the pollutants react directly on the anode’s surface by physisorbed ^{*}OH radicals produced by BDD. Indirect oxidation occurs through the electrochemical generation of a mediator in solution (such as Cl^{*}, Cl₂, or ClO⁻ and HClO). To generate active chlorine (Cl^{*}), dissolved Cl⁻ should be oxidized directly on the anode’s surface (Equation (8)). If the concentration of Cl₂ is exceeded, hypochlorous acid (HClO) can be generated (Equation (9)), which is in equilibrium with hypochlorite ions (ClO⁻) at a neutral pH (Equation (10)) [33]:



When a BDD anode is employed, more hydroxyl radicals are generated, which enhances the catalytic reaction of the radicals to oxidize chloride ions into different oxochlorinated compounds (Equations (11)–(14)) [45]. As described by [45], this significantly enhances the oxidation of the organic contaminants:



The destruction of heavy metals can be conducted on the anodic surface by either the anode directly or radical ^{*}OH. Anodic oxidation is described as follows: (1) transfer of the electron to the anode surface (M); (2) production of the powerful physisorbed radical ^{*}OH at the anode surface, signified by M (radical ^{*}OH), due to water or OH⁻ in the wastewater (Equation (15)); and (3) destruction of heavy metal (L) complexes by ^{*}OH and the depositing of heavy metals ions of the cathode (Equation (16)) [46]:



The abatement of pollutants via electro-ozonation is achieved by two different approaches: indirect oxidation, in which a mediator is electrochemically caused to perform oxidation; and direct anodic oxidation, in which pollutants are destroyed on the anode’s surface [30].

Some researchers [47] have stated that ozone can be considered as a good choice for removing emerging contaminants (such as antibiotics) from water bodies, and ECs can be promptly destroyed by ozone. Thus, to improve the oxidation and removal of ECs, ozonation was combined with electrochemical oxidation. In ozonation systems, ECs can be oxidized by direct reaction with ozone (Equation (17)). Furthermore, hydroxyl radicals can be generated through the decomposition of ozone (Equation (18)). Equation (19) shows the indirect reaction with non-selective and highly reactive hydroxyl radicals [48]:



Ozone is able to react with double or triple bonds (such as C=C, C=N, N=N, and C≡C) and break them. The mechanism of the mineralization of organic contaminants by ozonation is demonstrated in Figure 2 [49]. Moreover, Portjanskaja [50] stated that ozone can be useful in the elimination of soluble metals and in the decomplexing of bound heavy metals due to the strong oxidative properties of ozone.

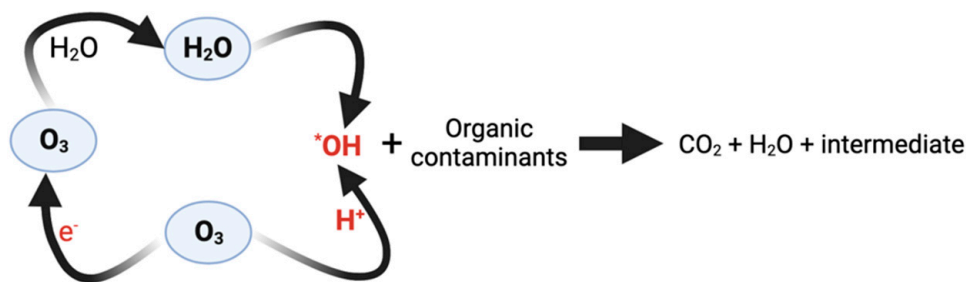


Figure 2. Mechanism of organic contaminant mineralization by ozonation (modified from [49], and permission for re-using the figure was received on 14 August 2022 from Elsevier).

The results of the first step of the study were optimized using RSM. Several studies [51,52] applied RSM and CCD to optimize pollutant removal from water bodies using different physicochemical and biological methods. RSM is known as a mathematical and statistical analysis approach, where the removal of pollutants (responses) is affected by several independent factors (variables) for analysis optimization [53]. A statistical analysis of the results in the current study is shown in Table 3. Based on Table 3, the high values of R² (>0.9) indicate that RSM can optimize the performance of the first step in a logical way. Furthermore, the final equations of TND, DMP, Ni, and Pb are displayed by Equations (20), (21), (22), and (23), respectively.

Table 3. Statistical analysis results for response parameters in RSM and ANN.

Reponses	R ² *	Adj. R ²	Adec. P	SD	CV
TND removal	0.943	0.934	36.50	3.01	5.60
DMP removal	0.937	0.903	33.27	3.18	5.11
Ni removal	0.915	0.901	25.52	3.29	7.73
Pb removal	0.919	0.906	25.60	3.24	7.82

* R²: R-squared; Adj. R²: adjusted R-squared; Adec. P: adequate precision; SD: std. dev.; CV: %.

A, B, C, and D are defined as the ozonation time (min), ozone dosage (mg L⁻¹), initial concentration of ECs (mg L⁻¹), and initial concentration of metals (mg L⁻¹), respectively.

The final equations in terms of coded factors are as below. In all equations, A, AB, and AC are significant model terms (in terms of Prob > F less than 0.05):

$$\text{Removal of TND} = 56.26 + 15.12A - 6.51AB + 7.35AC \tag{20}$$

$$\text{Removal of DMP} = 64.02 + 15.40A - 6.18AB + 6.17AC \tag{21}$$

$$\text{Removal of Ni} = 43.31 + 14.23A - 0.53AB + 2.29AC \tag{22}$$

$$\text{Removal of Pb} = 42.29 + 14.47A - 0.23AB + 2.28AC \tag{23}$$

As shown in Figures 3 and 4, the maximum removal of TND (77.0%), DMP (84.5%), Ni (59.2%), and Pb (58.2%) was reached at the optimum ozonation time of 58.1 min, the ozone dosage of 9.4 mg L⁻¹, the initial concentration of ECs of 0.98 mg L⁻¹, and the initial concentration of heavy metals of 28.9 mg L⁻¹. Figures 5 and 6 present design expert statistical plots, which show high agreement between predicted data and experimental data.

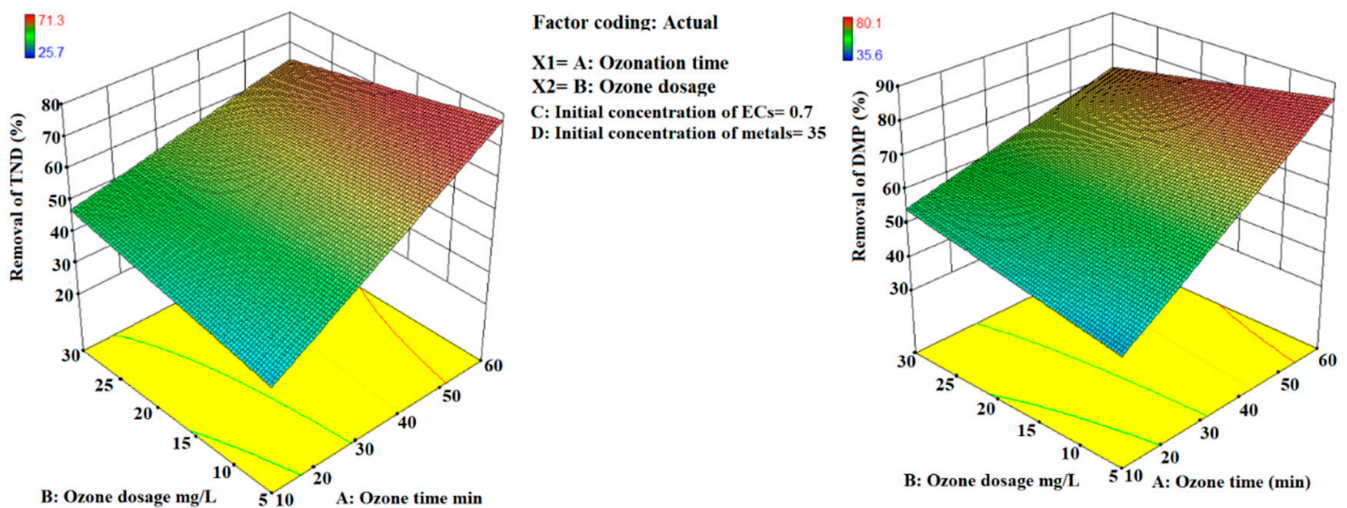


Figure 3. 3D surface plots for removal of TND and DMP.

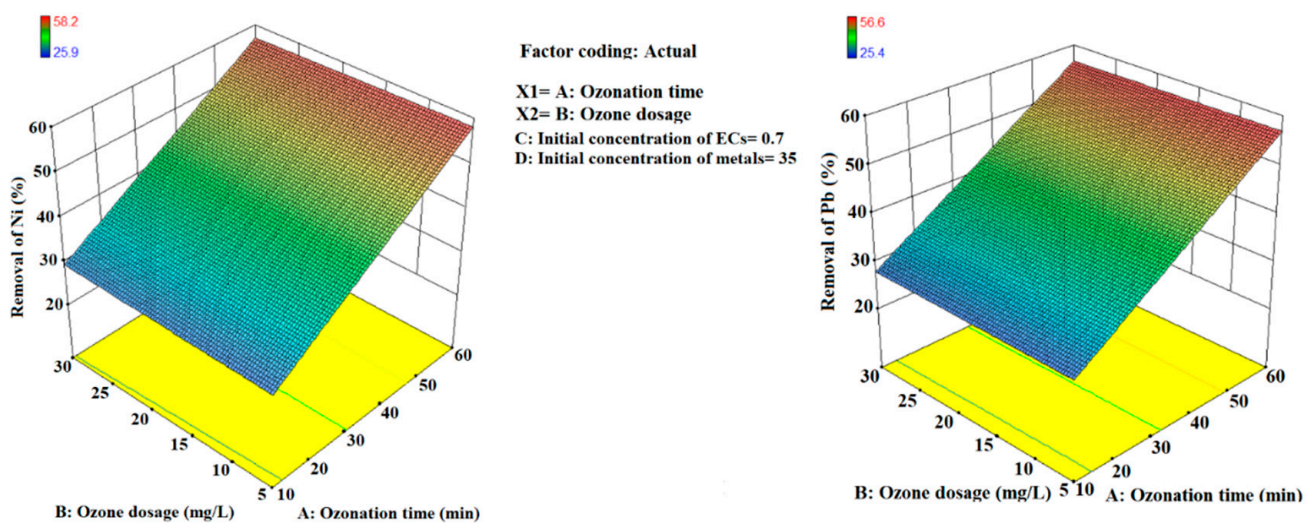


Figure 4. 3D surface plots for removal of Ni and Pb.

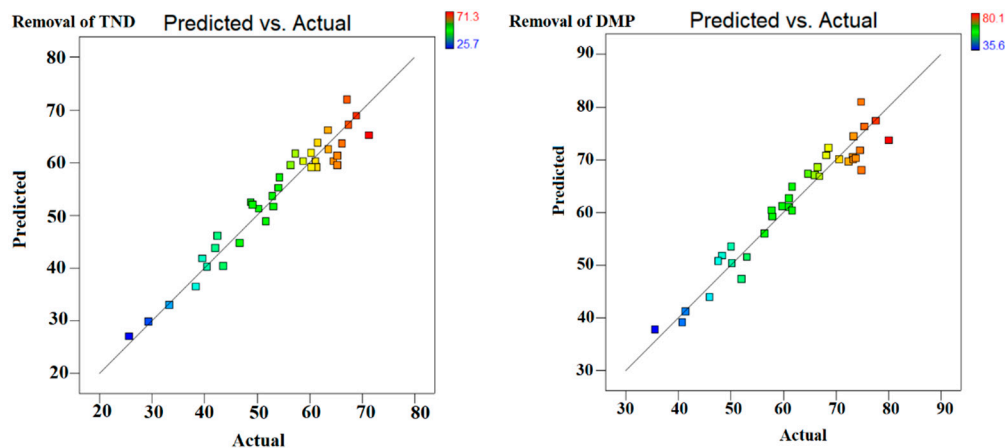


Figure 5. Design expert statistical plots for removal of TND and DMP.

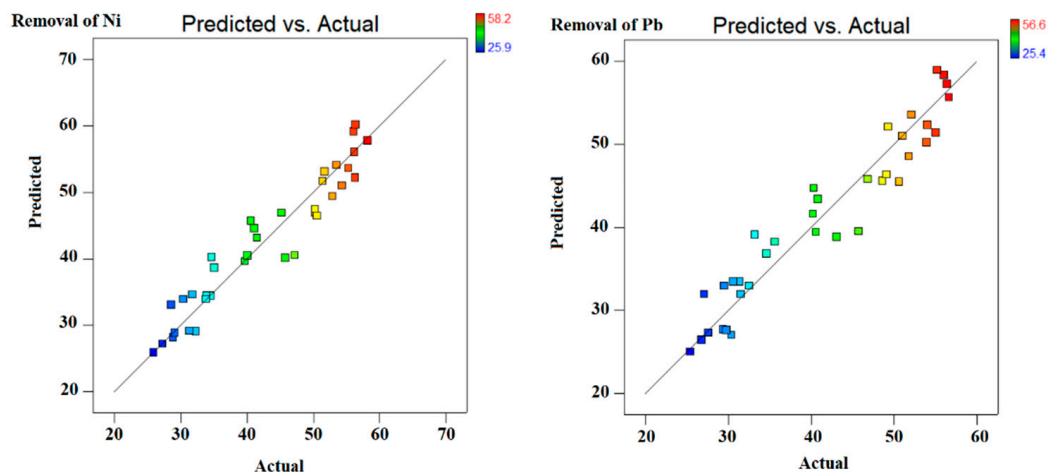


Figure 6. Design expert statistical plots for removal of Ni and Pb.

3.2. Ozone Consumption (OC) and Specific Energy Consumption (SEC)

In this study, ozone consumption (Equation (3)) specifies the amounts of ozone that can be applied to remove certain amounts of ECs [30]. OC is a vital factor in the ozone process due to its correlation with the operation costs [54]. Tizaoui et al. [54] reported an OC of 1.5 to 3.5 (kg O₃/kg COD) during the treatment of landfill leachate with a modified ozone reactor. Abu Amr et al. [55] reported an OC of more than 0.76 (kg O₃/kg COD) during landfill leachate treatment with zone reactors. The findings of the OC tests are presented in Table 4. Based on Table 4, the OC ranges from 1.11 to 3.95 (kg O₃/kg ECs), which is in agreement with the findings of previous studies. However, Abu Amr et al. [55] stated that the various OCs reported in the literature are mostly due to the variations in experimental conditions and wastewater characteristics (e.g., sample volume, O₃ dosage, and pH variation).

Table 4. Consumption of ozone at reaction times.

Reaction Time (min)	10	20	30	40	50	60
OC (kg O ₃ /kg ECs)	1.11	1.39	2.1	3.05	3.95	3.81

SEC has been applied by several researchers [56] to estimate energy consumption during the treatment of wastewater with electrochemical oxidation. Morsi et al. [56] reported an EC of 4.7 (kWh kg⁻¹) in the removal of dyes with electrochemical oxidation when the current was 30 mA. An SEC of 296 to 1676 (kWh kg⁻¹) was reported by

Murthy et al. [57] in the treatment of textile wastewater with EO when the current was 120 to 480 mA/cm². In the current study, the current and voltage were 30 mA/cm² and 9 V, respectively. Mojiri et al. [58] reported an SEC of 6.5 (kWh kg⁻¹) during the treatment of synthetic wastewater with EO. Therefore, based on Equation (4), the SEC was 6.9 for the removal of ECs with EO.

3.3. Removal of ECs and Heavy Metals with a Fixed-Bed Column and an Adsorption Isotherm

After the treatment of synthetic wastewater under optimum conditions, the wastewater was moved through a fixed-bed column, which was filled with BBCEC. After this step, 92.1% of TND and 99.9% of DMP, Ni, and Pb were removed. The BBCEC was integrated from different low-cost materials (including bentonite, biochar, cockleshells, eggshells, and cement). Therefore, pollutants can be removed by BBCEC via ion exchange and adsorption simultaneously. A total of 99% of DMP was removed with a combination of ozonation and cerium supported on activated carbon, with a 60 min ozonation time and an ozone dosage of 30 mg [41], which is in line with findings of the current study. Around 50% of TND was removed with combined adsorption and biodegradation [59]. A total of 73.4% of Ni was eliminated by the integration of an advanced oxidation process and adsorption [30].

Adsorption isotherms are vital characteristics for controlling the adsorption process, and the commonly applied isotherm models of the adsorption process are the Langmuir and Freundlich models [60]. Adsorption isotherms were measured in batch experiments under different concentrations of ECs (0.2 to 1.2 mg L⁻¹ and 10 to 60 mg L⁻¹), and varying adsorption dosages (1 to 50 g L⁻¹). The obtained plots and results are demonstrated in Figures S1 and S2 (in supplementary file) and in Table 5. For the adsorption of TND and DMP, the K_L values were 0.03 and 0.04, respectively, which is in line with findings of Marohan et al. [61]. For the Langmuir isotherm study, the R^2 for ECs and heavy metals was 0.89 to 0.81. The K_L values were 0.09 and 0.1 for the adsorption of Ni and Pb, respectively. An et al. [62] and Jin et al. [63] stated $K_L = 0.05$ and $K_L = 0.1$ for the adsorption of Ni and Pb with a biochar-based system, respectively, which is in agreement with the current study. For the removal of ECs with biochar-based adsorption, the Q_m (mg g⁻¹) ranged from 1.1 to 75.9 [64], which is in line with the current study. Moreover, for the elimination of heavy metals (Ni) with a biochar-based adsorbent, the Q_m (mg g⁻¹) was 24.6 [62], which is in accordance with the current study. For the Freundlich isotherm study, the R^2 values were 0.92, 0.95, 0.97, and 0.99 for the adsorption of TND, DMP, Ni, and Pb, respectively. Kozyatnyk et al. [64], An et al. [62], and Li et al. [65] reported $R^2 = 0.94$, $R^2 = 0.90$, and $R^2 = 0.92$ for the removal of ECs, Ni, and Pb from an aqueous solution with a biochar-based adsorbent, which is in agreement with the current study. Furthermore, the K_F (mg g⁻¹ (L/mg)^{1/n}) for TND, DMP, Ni, and Pb were 2.2, 2.9, 9.7, and 10.3, respectively, which is in accordance with findings of Kozyatnyk et al. [64].

Table 5. Details of Langmuir and Freundlich isotherm studies.

Pollutants	Langmuir			Freundlich		
	Q_m (mg g ⁻¹)	K_L	R^2	K_F (mg g ⁻¹ (L/mg) ^{1/n})	1/n	R^2
TND	13.1	0.03	0.897	2.2	0.54	0.920
DMP	17.2	0.04	0.872	2.9	0.60	0.951
Ni	21.4	0.07	0.812	9.7	0.26	0.975
Pb	20.7	0.09	0.840	10.3	1.11	0.995

It was revealed that the Freundlich isotherm is a better fit than the Langmuir for the removal of ECs and metals. This indicates that all sites on the BBCEC have equal affinity for the adsorbates [66]. The adsorption of ECs and heavy metals followed the Freundlich

isotherm; the high R^2 values indicate that the adsorption of ECs and metals occurred mostly due to chemical bonding [66].

4. Conclusions

An integrated system that included electro-ozonation and a fixed-bed column filled with a novel composite adsorbent (named BBCEC) was employed to remove TND, DMP, Ni, and Pb from synthetic wastewater. CCD and RSM were utilized to optimize the parameters. The main conclusions of the current research are discussed follows. Electro-ozonation could remove 77.0%, 84.5%, 59.2%, and 58.2% of TND, DMP, Ni, and Pb, respectively, at the optimum reaction time of 58.1 min, ozone dosage of 9.4 mg L⁻¹, initial concentration of ECs of 0.98 mg L⁻¹, and initial concentration of heavy metals of 28.9 mg L⁻¹. The ozone consumption (OC) varied from 1.1 kg to 3.9 kg (kg O₃/kg ECs), and the specific energy consumption (SEC) was 6.95 (kWh kg⁻¹). The performance of the combined electro-ozonation and fixed-bed column enhanced the efficiency of the removal of TND, DMP, Ni, and Pb to 92–99%. The removal of TND, DMP, Ni, and Pb with BBCEC is justified with the Freundlich isotherm better than the Langmuir isotherm.

Supplementary Materials: The following supporting information can be downloaded at: <https://www.mdpi.com/article/10.3390/separations9100276/s1>, Figure S1: plot for the Langmuir adsorption isotherm; Figure S2: Plot for the Freundlich adsorption isotherm.

Author Contributions: Conceptualization, A.M., J.L.Z. and N.O.; methodology, M.A.Z. and R.A.K.; software, R.A.K.; validation, S.R. and M.V.; investigation, M.A.Z., R.A.K. and S.G.; resources, H.F.; data curation, R.A.K. and H.F.; writing—original draft preparation, A.M.; writing—review A.M. and editing, J.L.Z.; funding acquisition, A.M. and N.O. All authors have read and agreed to the published version of the manuscript.

Funding: JSPS KAKENHI: grant number 21H01465, supported the study.

Data Availability Statement: Not applicable.

Conflicts of Interest: The authors declare no conflict of interest.

References

1. Lin, L.; Yang, H.; Xu, X. Effects of Water Pollution on Human Health and Disease Heterogeneity: A Review. *Front. Environ. Sci.* **2022**, *10*, 880246. [CrossRef]
2. Rajendran, S.; Priya, A.K.; Senthil Kumar, P.; Hoang, T.K.A.; Sekar, K.; Chong, K.Y.; Khoo, K.S.; Ng, H.S.; Show, P.L. A critical and recent developments on adsorption technique for removal of heavy metals from wastewater—A review. *Chemosphere* **2022**, *303*, 135146. [CrossRef] [PubMed]
3. Khan, S.; Naushad, M.; Govarthan, M.; Iqbal, J.; Alfadul, S.M. Emerging contaminants of high concern for the environment: Current trends and future research. *Environ. Res.* **2022**, *207*, 112609. [CrossRef] [PubMed]
4. Santiago-Morales, J.; Gómez, M.J.; Herrera, S.; Fernández-Alba, A.R.; García-Calvo, E.; Rosal, R. Oxidative and photochemical processes for the removal of galaxolide and tonalide from wastewater. *Water Res.* **2012**, *46*, 4435–4447. [CrossRef] [PubMed]
5. Rosal, R.; Rodríguez, A.; Perdigón-Melón, J.A.; Petre, A.; García-Calvo, E.; Gómez, M.J.; Agüera, A.; Fernández-Alba, A.R. Occurrence of emerging pollutants in urban wastewater and their removal through biological treatment followed by ozonation. *Water Res.* **2010**, *44*, 578–588. [CrossRef]
6. Košnář, Z.; Mercl, F.; Chane, A.D.; Pierdonà, L.; Míchal, P.; Tlustoš, P. Occurrence of synthetic polycyclic and nitro musk compounds in sewage sludge from municipal wastewater treatment plants. *Sci. Total Environ.* **2021**, *801*, 149777. [CrossRef]
7. Zhou, X.; Xiong, W.; Li, Y.; Zhang, C.; Xiong, X. A novel simultaneous coupling of memory photocatalysts and microbial communities for alternate removal of dimethyl phthalate and nitrate in water under light/dark cycles. *J. Hazard. Mater.* **2022**, *430*, 128395. [CrossRef]
8. Ding, S.; Wan, J.; Ma, Y.; Wang, Y.; Li, X.; Sun, J.; Pu, M. Targeted degradation of dimethyl phthalate by activating persulfate using molecularly imprinted Fe-MOF-74. *Chemosphere* **2021**, *270*, 128620. [CrossRef]
9. Zhang, L.; Zhao, B.; Xu, G.; Guan, Y. Characterizing fluvial heavy metal pollutions under different rainfall conditions: Implication for aquatic environment protection. *Sci. Total Environ.* **2018**, *635*, 1495–1506. [CrossRef]
10. Vakili, M.; Rafatullah, M.; Yuan, J.; Zwain, H.M.; Mojiri, A.; Gholami, Z.; Gholami, F.; Wang, W.; Giwa, A.S.; Yu, Y.; et al. Nickel ion removal from aqueous solutions through the adsorption process: A review. *Rev. Chem. Eng.* **2020**, *37*, 755–778. [CrossRef]

11. Rezania, S.; Mojiri, A.; Park, J.; Nawrot, N.; Wojciechowska, E.; Marraiki, N.; Zaghoul, N.S.S. Removal of lead ions from wastewater using lanthanum sulfide nanoparticle decorated over magnetic graphene oxide. *Environ. Res.* **2022**, *204*, 111959. [[CrossRef](#)] [[PubMed](#)]
12. Mojiri, A.; Aziz, H.A.; Zaman, N.Q.; Aziz, S.Q.; Zahed, M.A. Metals removal from municipal landfill leachate and wastewater using adsorbents combined with biological method. *Desalin. Water Treat.* **2016**, *57*, 2819–2833. [[CrossRef](#)]
13. Vakili, M.; Mojiri, A.; Kindaichi, T.; Cagnetta, G.; Yuan, J.; Wang, B.; Giwa, A.S. Cross-linked chitosan/zeolite as a fixed-bed column for organic micropollutants removal from aqueous solution, optimization with RSM and artificial neural network. *J. Environ. Manag.* **2019**, *250*, 109434. [[CrossRef](#)] [[PubMed](#)]
14. Chen, G.; Dong, W.; Wang, H.; Zhao, Z.; Wang, F.; Wang, F.; Nieto-Delgado, C. Carbamazepine degradation by visible-light-driven photocatalyst Ag₃PO₄/GO: Mechanism and pathway. *Environ. Sci. Ecotechnology* **2022**, *9*, 100143. [[CrossRef](#)] [[PubMed](#)]
15. Joseph, C.G.; Farm, Y.Y.; Taufiq-Yap, Y.H.; Pang, C.K.; Nga, J.L.H.; Li Puma, G. Ozonation treatment processes for the remediation of detergent wastewater: A comprehensive review. *J. Environ. Chem. Eng.* **2021**, *9*, 106099. [[CrossRef](#)]
16. Fraiese, A.; Naddeo, V.; Uyguner-Demirel, C.S.; Prado, M.; Cesaro, A.; Zarra, T.; Liu, H.; Belgiorno, V.; Ballesteros, F., Jr. Removal of Emerging Contaminants in Wastewater by Sonolysis, Photocatalysis and Ozonation. *Glob. NEST J.* **2018**, *21*, 98–105. [[CrossRef](#)]
17. Gomes, J.; Costa, R.; Quinta-Ferreira, R.M.; Martins, R.C. Application of ozonation for pharmaceuticals and personal care products removal from water. *Sci. Total Environ.* **2017**, *586*, 265–283. [[CrossRef](#)]
18. Ghosh, S.; Falyouna, O.; Malloum, A.; Othmani, A.; Bornman, C.; Bedair, H.; Onyeaka, H.; Al-Sharify, Z.T.; Jacob, A.O.; Miri, T.; et al. A general review on the use of advance oxidation and adsorption processes for the removal of furfural from industrial effluents. *Microporous Mesoporous Mater.* **2022**, *331*, 111638. [[CrossRef](#)]
19. Kwarciak-Kozłowska, A. Removal of pharmaceuticals and personal care products by ozonation, advance oxidation processes, and membrane separation. In *Pharmaceuticals and Personal Care Products: Waste Management and Treatment Technology*; Elsevier: Amsterdam, The Netherlands, 2019; pp. 151–171.
20. Alfonso-Muniozguren, P.; Cotillas, S.; Boaventura, R.A.R.; Moreira, F.C.; Lee, J.; Vilar, V.J.P. Single and combined electrochemical oxidation driven processes for the treatment of slaughterhouse wastewater. *J. Clean. Prod.* **2020**, *270*, 121858. [[CrossRef](#)]
21. Yang, C.; Jin, X.; Hu, S.; Guo, Y.; Qian, Z.; Jin, P. Enhanced removal of organics and ammonia by a composite anode in the electrochemically assisted ozonation (EAO) processes with reduced sludge and alleviated passivation. *Sep. Purif. Technol.* **2022**, *297*, 121536. [[CrossRef](#)]
22. Haciosmanoğlu, G.G.; Mejías, C.; Martín, J.; Santos, J.L.; Aparicio, I.; Alonso, E. Antibiotic adsorption by natural and modified clay minerals as designer adsorbents for wastewater treatment: A comprehensive review. *J. Environ. Manag.* **2022**, *317*, 115397. [[CrossRef](#)] [[PubMed](#)]
23. Thotagamuge, R.; Kooch, M.R.R.; Mahadi, A.H.; Lim, C.M.; Abu, M.; Jan, A.; Hanipah, A.H.A.; Khiong, Y.Y.; Shofry, A. Copper modified activated bamboo charcoal to enhance adsorption of heavy metals from industrial wastewater. *Environ. Nanotechnol. Monit. Manag.* **2021**, *16*, 100562. [[CrossRef](#)]
24. Suhaimi, N.; Kooch, M.R.R.; Lim, C.M.; Chou Chao, C.-T.; Chou Chau, Y.-F.; Mahadi, A.H.; Chiang, H.-P.; Haji Hassan, N.H.; Thotagamuge, R. The Use of Gigantochloa Bamboo-Derived Biochar for the Removal of Methylene Blue from Aqueous Solution. *Adsorpt. Sci. Technol.* **2022**, *2022*, 1–12. [[CrossRef](#)]
25. Mojiri, A.; Aziz, H.A.; Zaman, N.Q.; Aziz, S.Q.; Zahed, M.A. Powdered ZELIAC augmented sequencing batch reactors (SBR) process for co-treatment of landfill leachate and domestic wastewater. *J. Environ. Manag.* **2014**, *139*, 1–14. [[CrossRef](#)] [[PubMed](#)]
26. Mokokwe, G.; Letshwenyo, M.W. Utilisation of cement brick waste as low cost adsorbent for the adsorptive removal of copper, nickel and iron from aqueous solution: Batch and column studies. *Phys. Chem. Earth Parts A/B/C* **2022**, *126*, 103156. [[CrossRef](#)]
27. Ngana, B.N.; Seumo, P.M.T.; Sambang, L.M.; Dedzo, G.K.; Nansu-Njiki, C.P.; Ngameni, E. Grafting of reactive dyes onto lignocellulosic material: Application for Pb(II) adsorption and electrochemical detection in aqueous solution. *J. Environ. Chem. Eng.* **2021**, *9*, 104984. [[CrossRef](#)]
28. Huang, J.; Zimmerman, A.R.; Chen, H.; Wan, Y.; Zheng, Y.; Yang, Y.; Zhang, Y.; Gao, B. Fixed bed column performance of Al-modified biochar for the removal of sulfamethoxazole and sulfapyridine antibiotics from wastewater. *Chemosphere* **2022**, *305*, 135475. [[CrossRef](#)]
29. Mojiri, A.; Vakili, M.; Farraji, H.; Aziz, S.Q. Combined ozone oxidation process and adsorption methods for the removal of acetaminophen and amoxicillin from aqueous solution; kinetic and optimisation. *Environ. Technol. Innov.* **2019**, *15*, 100404. [[CrossRef](#)]
30. Mojiri, A.; Ziyang, L.; Hui, W.; Ahmad, Z.; Tajuddin, R.M.; Abu Amr, S.S.; Kindaichi, T.; Aziz, H.A.; Farraji, H. Concentrated landfill leachate treatment with a combined system including electro-ozonation and composite adsorbent augmented sequencing batch reactor process. *Process Saf. Environ. Prot.* **2017**, *111*, 253–262. [[CrossRef](#)]
31. Du, X.; Mo, Z.; Li, Z.; Zhang, W.; Luo, Y.; Nie, J.; Wang, Z.; Liang, H. Boron-doped diamond (BDD) electro-oxidation coupled with nanofiltration for secondary wastewater treatment: Antibiotics degradation and biofouling. *Environ. Int.* **2021**, *146*, 106291. [[CrossRef](#)]
32. Wachter, N.; Aquino, J.M.; Denadai, M.; Barreiro, J.C.; Silva, A.J.; Cass, Q.B.; Bocchi, N.; Rocha-Filho, R.C. Electrochemical degradation of the antibiotic ciprofloxacin in a flow reactor using distinct BDD anodes: Reaction kinetics, identification and toxicity of the degradation products. *Chemosphere* **2019**, *234*, 461–470. [[CrossRef](#)] [[PubMed](#)]

33. García-Espinoza, J.D.; Mijaylova-Nacheva, P.; Avilés-Flores, M. Electrochemical carbamazepine degradation: Effect of the generated active chlorine, transformation pathways and toxicity. *Chemosphere* **2018**, *192*, 142–151. [[CrossRef](#)] [[PubMed](#)]
34. Aziz, S.Q.; Aziz, H.A.; Yusoff, M.S.; Bashir, M.J.K. Landfill leachate treatment using powdered activated carbon augmented sequencing batch reactor (SBR) process: Optimization by response surface methodology. *J. Hazard. Mater.* **2011**, *189*, 404–413. [[CrossRef](#)] [[PubMed](#)]
35. Gonzaga, I.M.D.; Moratalla, A.; Eguiluz, K.I.B.; Salazar-Banda, G.R.; Cañizares, P.; Rodrigo, M.A.; Saez, C. Influence of the doping level of boron-doped diamond anodes on the removal of penicillin G from urine matrixes. *Sci. Total Environ.* **2020**, *736*, 139536. [[CrossRef](#)]
36. Vakili, M.; Mojiri, A.; Zwain, H.M.; Yuan, J.; Giwa, A.S.; Wang, W.; Gholami, F.; Guo, X.; Cagnetta, G.; Yu, G. Effect of beading parameters on cross-linked chitosan adsorptive properties. *React. Funct. Polym.* **2019**, *144*, 104354. [[CrossRef](#)]
37. Mojiri, A.; Zhou, J.L.; Nazari, V.M.; Rezania, S.; Farraji, H.; Vakili, M. Biochar enhanced the performance of microalgae/bacteria consortium for insecticides removal from synthetic wastewater. *Process Saf. Environ. Prot.* **2022**, *157*, 284–296. [[CrossRef](#)]
38. Hernández-Leal, L.; Temmink, H.; Zeeman, G.; Buisman, C.J.N. Removal of micropollutants from aerobically treated grey water via ozone and activated carbon. *Water Res.* **2011**, *45*, 2887–2896. [[CrossRef](#)]
39. Mishra, S.; Srivastava, S.; Tripathi, R.D.; Kumar, R.; Seth, C.S.; Gupta, D.K. Lead detoxification by coontail (*Ceratophyllum demersum* L.) involves induction of phytochelatins and antioxidant system in response to its accumulation. *Chemosphere* **2006**, *65*, 1027–1039. [[CrossRef](#)]
40. Ternes, T.A.; Stüber, J.; Herrmann, N.; McDowell, D.; Ried, A.; Kampmann, M.; Teiser, B. Ozonation: A tool for removal of pharmaceuticals, contrast media and musk fragrances from wastewater? *Water Res.* **2003**, *37*, 1976–1982. [[CrossRef](#)]
41. Li, L.; Ye, W.; Zhang, Q.; Sun, F.; Lu, P.; Li, X. Catalytic ozonation of dimethyl phthalate over cerium supported on activated carbon. *J. Hazard. Mater.* **2009**, *170*, 411–416. [[CrossRef](#)]
42. Wang, J.; Zhou, Y.; Zhu, W.; He, X. Catalytic ozonation of dimethyl phthalate and chlorination disinfection by-product precursors over Ru/AC. *J. Hazard. Mater.* **2009**, *166*, 502–507. [[CrossRef](#)] [[PubMed](#)]
43. Kanakaraju, D.; Glass, B.D.; Oelgemöller, M. Advanced oxidation process-mediated removal of pharmaceuticals from water: A review. *J. Environ. Manag.* **2018**, *219*, 189–207. [[CrossRef](#)] [[PubMed](#)]
44. Lan, Y.; Coetsier, C.; Causserand, C.; Groenen Serrano, K. An experimental and modelling study of the electrochemical oxidation of pharmaceuticals using a boron-doped diamond anode. *Chem. Eng. J.* **2018**, *333*, 486–494. [[CrossRef](#)]
45. Martínez-Cruz, A.; Fernandes, A.; Ciriaco, L.; Pacheco, M.J.; Carvalho, F.; Afonso, A.; Madeira, L.; Luz, S.; Lopes, A. Electrochemical Oxidation of Effluents from Food Processing Industries: A Short Review and a Case-Study. *Water* **2020**, *12*, 3546. [[CrossRef](#)]
46. Du, J.; Zhang, B.; Li, J.; Lai, B. Decontamination of heavy metal complexes by advanced oxidation processes: A review. *Chin. Chem. Lett.* **2020**, *31*, 2575–2582. [[CrossRef](#)]
47. Rame, R.; Pranoto, H.; Winahyu, R.; Sofie, M.; Raharjo, B.; Utomo, A. Catalytic Ozonation Based Advanced Oxidation Process for Effective Treating Wastewater from Hospital and Community Health Centre Facility by FLASH WWT Catalyst System in Indonesia. *J. Phys. Conf. Ser.* **2018**, *1095*, 12030. [[CrossRef](#)]
48. Hansen, K.M.S.; Spiliotopoulou, A.; Chhetri, R.K.; Escolà Casas, M.; Bester, K.; Andersen, H.R. Ozonation for source treatment of pharmaceuticals in hospital wastewater—Ozone lifetime and required ozone dose. *Chem. Eng. J.* **2016**, *290*, 507–514. [[CrossRef](#)]
49. M’Arimi, M.M.; Mecha, C.A.; Kiprop, A.K.; Ramkat, R. Recent trends in applications of advanced oxidation processes (AOPs) in bioenergy production: Review. *Renew. Sustain. Energy Rev.* **2020**, *121*, 109669. [[CrossRef](#)]
50. Portjanskaja, E. *Ozone Science and Technology—Ozone reactions with Inorganic and Organic Compounds in Water*; Encyclopedia of Life Support System (EOLSS): Paris, France, 2010; p. 27.
51. Rifi, S.K.; Souabi, S.; El Fels, L.; Driouich, A.; Nassri, I.; Haddaji, C.; Hafidi, M. Optimization of coagulation process for treatment of olive oil mill wastewater using *Moringa oleifera* as a natural coagulant, CCD combined with RSM for treatment optimization. *Process Saf. Environ. Prot.* **2022**, *162*, 406–418. [[CrossRef](#)]
52. Bajpai, M.; Katoch, S.S.; Kadier, A.; Ma, P.-C. Treatment of pharmaceutical wastewater containing cefazolin by electrocoagulation (EC): Optimization of various parameters using response surface methodology (RSM), kinetics and isotherms study. *Chem. Eng. Res. Des.* **2021**, *176*, 254–266. [[CrossRef](#)]
53. Abdulgader, M.; Yu, Q.J.; Zinatizadeh, A.A.; Williams, P.; Rahimi, Z. Application of response surface methodology (RSM) for process analysis and optimization of milk processing wastewater treatment using multistage flexible fiber biofilm reactor. *J. Environ. Chem. Eng.* **2020**, *8*, 103797. [[CrossRef](#)]
54. Tizaoui, C.; Bouselmi, L.; Mansouri, L.; Ghrabi, A. Landfill leachate treatment with ozone and ozone/hydrogen peroxide systems. *J. Hazard. Mater.* **2007**, *140*, 316–324. [[CrossRef](#)]
55. Abu Amr, S.S.; Aziz, H.A.; Adlan, M.N.; Bashir, M.J.K. Pretreatment of stabilized leachate using ozone/persulfate oxidation process. *Chem. Eng. J.* **2013**, *221*, 492–499. [[CrossRef](#)]
56. Morsi, M.S.; Al-Sarawy, A.A.; El-Dein, W.A.S. Electrochemical degradation of some organic dyes by electrochemical oxidation on a Pb/PbO₂ electrode. *Desalin. Water Treat.* **2011**, *26*, 301–308. [[CrossRef](#)]
57. Usha, U.N.; Rekha, H.B.; Bhavya, J.G.B. Performance of Electrochemical Oxidation in Treating Textile Dye Wastewater by Stainless Steel Anode. *Int. J. Environ. Sci. Dev.* **2011**, *2*, 484.

58. Mojiri, A.; Ohashi, A.; Ozaki, N.; Kindaichi, T. Pollutants removal from synthetic wastewater by the combined electrochemical, adsorption and sequencing batch reactor (SBR). *Ecotoxicol. Environ. Saf.* **2018**, *161*, 137–144. [[CrossRef](#)]
59. Tasselli, S.; Valenti, E.; Guzzella, L. Polycyclic musk fragrance (PMF) removal, adsorption and biodegradation in a conventional activated sludge wastewater treatment plant in Northern Italy. *Environ. Sci. Pollut. Res.* **2021**, *28*, 38054–38064. [[CrossRef](#)]
60. Ru, J.; Wang, X.; Wang, F.; Cui, X.; Du, X.; Lu, X. UiO series of metal-organic frameworks composites as advanced sorbents for the removal of heavy metal ions: Synthesis, applications and adsorption mechanism. *Ecotoxicol. Environ. Saf.* **2021**, *208*, 111577. [[CrossRef](#)]
61. Manoharan, T.; Ganeshalingam, S.; Nadarajah, K. Mechanisms of emerging contaminants removal by novel neem chip biochar. *Environ. Adv.* **2022**, *7*, 100158. [[CrossRef](#)]
62. An, Q.; Jin, N.; Deng, S.; Zhao, B.; Liu, M.; Ran, B.; Zhang, L. Ni(II), Cr(VI), Cu(II) and nitrate removal by the co-system of *Pseudomonas hibiscicola* strain L1 immobilized on peanut shell biochar. *Sci. Total Environ.* **2022**, *814*, 152635. [[CrossRef](#)]
63. Jin, Q.; Wang, Z.; Feng, Y.; Kim, Y.-T.; Stewart, A.C.; O'Keefe, S.F.; Neilson, A.P.; He, Z.; Huang, H. Grape pomace and its secondary waste management: Biochar production for a broad range of lead (Pb) removal from water. *Environ. Res.* **2020**, *186*, 109442. [[CrossRef](#)] [[PubMed](#)]
64. Kozyatnyk, I.; Oesterle, P.; Wurzer, C.; Mašek, O.; Jansson, S. Removal of contaminants of emerging concern from multicomponent systems using carbon dioxide activated biochar from lignocellulosic feedstocks. *Bioresour. Technol.* **2021**, *340*, 125561. [[CrossRef](#)] [[PubMed](#)]
65. Li, Y.; Shaheen, S.M.; Azeem, M.; Zhang, L.; Feng, C.; Peng, J.; Qi, W.; Liu, J.; Luo, Y.; Peng, Y.; et al. Removal of lead (Pb²⁺) from contaminated water using a novel MoO₃-biochar composite: Performance and mechanism. *Environ. Pollut.* **2022**, *308*, 119693. [[CrossRef](#)] [[PubMed](#)]
66. Al Ali, A.; Ouda, M.; Naddeo, V.; Puig, S.; Hasan, S.W. Integrated electrochemical-adsorption process for the removal of trace heavy metals from wastewater. *Case Stud. Chem. Environ. Eng.* **2021**, *4*, 100147. [[CrossRef](#)]